

## Scaling properties in bulk and $p_T$ -dependent particle production near midrapidity in relativistic heavy ion collisions

B. Alver,<sup>1</sup> B. B. Back,<sup>2</sup> M. D. Baker,<sup>3</sup> M. Ballintijn,<sup>1</sup> D. S. Barton,<sup>3</sup> R. R. Betts,<sup>4</sup> R. Bindel,<sup>5</sup> W. Busza,<sup>1</sup> Z. Chai,<sup>3</sup> V. Chetluru,<sup>4</sup> E. García,<sup>4</sup> T. Gburek,<sup>6</sup> K. Gulbrandsen,<sup>1</sup> J. Hamblen,<sup>7</sup> I. Harnarine,<sup>4</sup> C. Henderson,<sup>1</sup> D. J. Hofman,<sup>4</sup> R. S. Hollis,<sup>4</sup> R. Hołyński,<sup>6</sup> B. Holzman,<sup>3</sup> A. Iordanova,<sup>4</sup> J. L. Kane,<sup>1</sup> P. Kulinich,<sup>1</sup> C. M. Kuo,<sup>8</sup> W. Li,<sup>1</sup> W. T. Lin,<sup>8</sup> C. Loizides,<sup>1</sup> S. Manly,<sup>7</sup> A. C. Mignerey,<sup>5</sup> R. Nouicer,<sup>4</sup> A. Olszewski,<sup>6</sup> R. Pak,<sup>3</sup> C. Reed,<sup>1</sup> E. Richardson,<sup>5</sup> C. Roland,<sup>1</sup> G. Roland,<sup>1</sup> J. Sagerer,<sup>4</sup> I. Sedykh,<sup>3</sup> C. E. Smith,<sup>4</sup> M. A. Stankiewicz,<sup>3</sup> P. Steinberg,<sup>3</sup> G. S. F. Stephens,<sup>1</sup> A. Sukhanov,<sup>3</sup> A. Szostak,<sup>3</sup> M. B. Tonjes,<sup>5</sup> A. Trzupek,<sup>6</sup> G. J. van Nieuwenhuizen,<sup>1</sup> S. S. Vaurynovich,<sup>1</sup> R. Verrier,<sup>1</sup> G. Veres,<sup>1</sup> P. Walters,<sup>7</sup> E. Wenger,<sup>1</sup> D. Willhelm,<sup>5</sup> F. L. H. Wolfs,<sup>7</sup> B. Wosiek,<sup>6</sup> K. Woźniak,<sup>6</sup> S. Wyngaardt,<sup>3</sup> and B. Wysłouch<sup>1</sup>

(PHOBOS Collaboration)

<sup>1</sup>Laboratory for Nuclear Science, Massachusetts Institute of Technology, Cambridge, Massachusetts 02139-4307, USA

<sup>2</sup>Physics Division, Argonne National Laboratory, Argonne, Illinois 60439-4843, USA

<sup>3</sup>Chemistry and C-A Departments, Brookhaven National Laboratory, Upton, New York 11973-5000, USA

<sup>4</sup>Department of Physics, University of Illinois at Chicago, Chicago, Illinois 60607-7059, USA

<sup>5</sup>Department of Chemistry, University of Maryland, College Park, Maryland 20742, USA

<sup>6</sup>Institute of Nuclear Physics PAN, Kraków, Poland

<sup>7</sup>Department of Physics and Astronomy, University of Rochester, Rochester, New York 14627, USA

<sup>8</sup>Department of Physics, National Central University, Chung-Li, Taiwan

(Received 13 August 2008; published 20 July 2009)

The centrality dependence of the midrapidity charged-particle multiplicity density ( $|\eta| < 1$ ) is presented for Au + Au and Cu + Cu collisions at RHIC over a broad range of collision energies. The multiplicity measured in the Cu + Cu system is found to be similar to that measured in the Au + Au system, for an equivalent  $N_{\text{part}}$ , with the observed factorization in energy and centrality still persistent in the smaller Cu + Cu system. The extent of the similarities observed for bulk particle production is tested by a comparative analysis of the inclusive transverse momentum distributions for Au + Au and Cu + Cu collisions near midrapidity. It is found that, within the uncertainties of the data, the ratio of yields between the various energies for both Au + Au and Cu + Cu systems are similar and constant with centrality, both in the bulk yields and as a function of  $p_T$ , up to at least 4 GeV/c. The effects of multiple nucleon collisions that strongly increase with centrality and energy appear to only play a minor role in bulk and intermediate transverse momentum particle production.

DOI: [10.1103/PhysRevC.80.011901](https://doi.org/10.1103/PhysRevC.80.011901)

PACS number(s): 25.75.Dw, 25.75.Ag

The experimental program at the Relativistic Heavy-Ion Collider (RHIC) at Brookhaven National Laboratory has opened a new era in the study of QCD matter. Measurements of the midrapidity density of charged particles have, from the start of the RHIC program, provided an estimate of the energy density created in these collisions as well as an important baseline against which to test core features of particle production in models. The wealth of data on bulk charged-particle production collected in the first five years of RHIC operations has revealed the presence of various features in the data that appear to be universal, including a factorization of the charged-particle production into two components, one that depends on collision energy, or  $\sqrt{s_{NN}}$ , and the other on the centrality of the colliding heavy ions [1]. The energy dependence of the midrapidity charged-particle density appears to be consistent with a logarithmic rise with  $\sqrt{s_{NN}}$  [2]. This logarithmic dependence resembles that in elementary  $p + p$  and  $e^+ + e^-$  collisions [3] and was not *a priori* expected for relativistic heavy ion collisions. In particular, initial expectations of a large increase in particle production with collision energy for central heavy ion collisions from multiple binary nucleon scatterings and the increased formation of mini-jets were not realized. Further studies revealed a relatively weak dependence of the produced midrapidity charged-particle multiplicity

density per participant pair on the collision centrality. From a two-component picture [4], the part of the multiplicity that scales with the number of binary collisions ( $N_{\text{coll}}$ ) contributes at the level of only  $\approx 13\%$ , across all energies studied so far at RHIC [5,6].

This Rapid Communication reports results from RHIC for the midrapidity charged-particle density in Cu + Cu collisions at  $\sqrt{s_{NN}} = 22.4, 62.4, \text{ and } 200$  GeV as a function of centrality. The data correspond to the top 50% of the total inelastic cross section and range from an average number of participating nucleons  $\langle N_{\text{part}} \rangle = 20$  to 108. The previously published study of the centrality dependence of Au + Au multiplicity also covered the top 50% of the total inelastic cross section, corresponding to  $\langle N_{\text{part}} \rangle > 60$ . Thus, the full investigation of bulk charged-particle production as a function of  $N_{\text{part}}$  was limited by the wide gap between the results of  $p + p$  collisions and the lowest measured Au + Au centrality bin. For Au + Au, this left room for different scenarios of particle production evolution in heavy ions and made it impossible to distinguish various evolution scenarios (for example, a smooth rise or a sudden jump at low  $N_{\text{part}}$  values). One way to circumvent this is via a detailed mapping of the particle production as a function of  $N_{\text{part}}$ , from values corresponding to mid-central Au + Au collisions all the way down to those

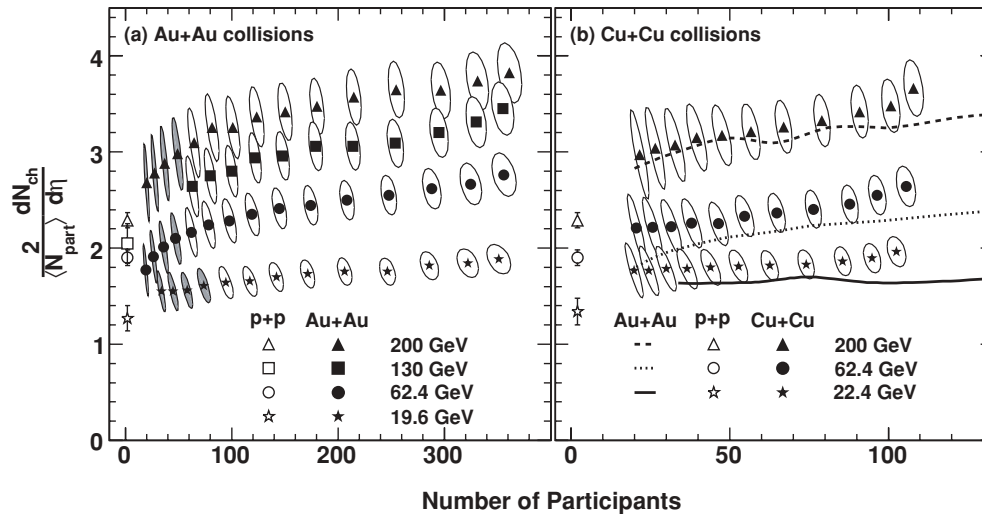


FIG. 1. The charged-particle pseudorapidity density at midrapidity ( $|\eta| < 1$ ), scaled by the number of participating nucleon pairs, for (a) Au + Au collisions and (b) Cu + Cu collisions. The shaded ellipses in panel (a) represent the uncertainty on the new peripheral data; unshaded ellipses are from Ref. [7]. In panel (b), the lines represent the Au + Au data (no errors) for comparison, where the 19.6-GeV data are scaled by 1.055 to account for the difference in collision energy from 22.4 GeV for the Cu + Cu data. The open symbols at  $N_{\text{part}} = 2$  represent the inelastic  $p + p$  data at equivalent energies to the data, as in Ref. [6]. The ellipses represent 90% C.L. systematic errors.

in  $d + Au$  collisions. The Cu + Cu data are therefore ideally suited for this study as the average number of participants in the most central data class ( $\langle N_{\text{part}}^{\text{max}} \rangle = 108$ ) overlaps with the peripheral Au + Au measurements, and the average number of participants in the most peripheral bin ( $\langle N_{\text{part}}^{\text{min}} \rangle = 20$ ) reaches down to the upper limit for central  $d + Au$  collisions. In addition, for the same number of participants as in Au + Au collisions, the relative uncertainty in the fractional cross section of Cu + Cu collisions is smaller, enabling a more precise measurement. Also discussed here is a subsequent reanalysis of the Au + Au data, using the techniques developed for Cu + Cu data analysis, that extends the overlap in  $N_{\text{part}}$  down to  $\sim 20$  participants. To compare the lowest energy Cu + Cu (22.4 GeV) and Au + Au (19.6 GeV) data [Fig. 1(b) and Fig. 2(b)], a multiplicative scaling factor was applied to the Au + Au data (1.055) that accounts for the small difference in the collision energy. This factor was derived from a fit to central  $A + A$  multiplicity data, at midrapidity, from AGS, SPS, and RHIC [7] results.

The new Cu + Cu collision data were recorded by the PHOBOS experiment during the 2005 RHIC run. The primary hardware triggering was performed, as in prior PHOBOS heavy ion data [1], by two sets of 16 scintillator “Paddle” counter arrays that cover a pseudorapidity of  $3.2 < |\eta| < 4.5$  ( $\eta = -\ln[\tan(\theta/2)]$ ). The read-out from the full PHOBOS detector was initiated by the occurrence of one or more scintillator hits on each array within  $\Delta t < 10$  ns. This trigger prevents the loss of central collision events that may occur for Cu + Cu collisions if the primary hardware trigger is based solely on the zero-degree calorimeters (ZDCs), which detect spectator neutrons. For this analysis, the energy and time information from the ZDCs were used as an additional hardware cross-check to remove any contamination from beam-gas background events for mid-central collisions. The resultant data were then passed through a series of off-line

quality checks before the physics analysis. The two most important of these checks include a cut on events with a time difference, between the Paddles, of 5 ns or less to filter out beam-gas collisions and a further cut on events that had a valid reconstructed primary vertex, determined as detailed in the following, within 10 cm of the nominal collision position.

The primary algorithms for vertex reconstruction in PHOBOS were initially optimized for high-multiplicity, central Au + Au collisions. For the Cu + Cu data, where multiplicity on average is much lower, the nominal reconstruction procedures are found to be inefficient, even for mid-central data. To maximize the usability of this dataset, two new vertex reconstruction techniques were designed to allow for the analysis of the more peripheral events. The first method finds the vertex position from hits in the single-layer Octagon detector ( $|\eta| < 3.2$ ) using a probabilistic approach applied to the energy deposited at each hit [8]. The overall vertex resolution attained by this technique is found to be  $\sigma \approx 0.6\text{--}1.0$  cm, dependent on the multiplicity of a given event. To obtain a better resolution along the beam axis ( $z$ ), a complementary method based on all possible two-point straight tracks is used. Straight line trajectories are assumed as the magnetic field in the region of the Vertex detector or the inner six planes of the Spectrometer (used in the vertex reconstruction) is negligible [9]. If the two-point track, formed from the Vertex detector and the first two silicon layers of the Spectrometer, passes close to the  $(x, y)$  orbit position of the beam, then the  $z$ -coordinate at the orbit position is considered a candidate for the collision vertex. From this ensemble of tracks, the  $z$ -position is determined from the most frequently found position. As a quality assurance measure, it is required that these two (independent) vertex positions are within  $|\Delta z| < 3$  cm of each other. This requirement removes all misidentified collision vertices without detriment to the efficiency. Agreement to within 3 cm represents a  $3\sigma$

acceptance of the lower resolution Octagon-based vertex. The overall vertex resolution for this procedure is determined by the two-point track vertex reconstruction method and is found to be  $\sigma < 0.1$  cm for high-multiplicity events and  $\sigma \sim 0.25$  cm for low-multiplicity data. This overall improvement in vertex reconstruction efficiency, while still maintaining a good resolution, has allowed all track-based analyses (including those reported here) to be carried out in the Cu + Cu collision system.

To provide a measure of the centrality of the collision, and subsequent assignment of model-based parameters such as the number of participants, the data are divided into bins of fractional cross section. These bins allow for the comparison of data between collision systems and energies. The first step toward determining the cross-section binning is to estimate the trigger and vertex reconstruction efficiency. Two methods were employed for the Cu + Cu data. The ‘‘Paddle hit’’ method counts the number of scintillator Paddle slats hit and compares them to the number from a fully simulated Monte Carlo (MC) sample of events. This method was also used in the analysis of 62.4–200 GeV Au + Au data. The inefficiency is estimated from the loss of events in the region of lowest number of Paddle slats hit (see, for example, Ref. [1]). A second technique, employed for both 19.6-GeV Au + Au and 200-GeV  $d$  + Au collisions, known as the shape-matching method, compares the distribution of hit multiplicity in the Octagon detector to that in the MC simulation [6]. The MC distribution is scaled to match the maximum multiplicity in data (under the assumption of 100% efficiency at maximum multiplicity) such that a ratio of the multiplicity distributions in data and in MC corresponds to the efficiency. Both of these techniques were used with two different MC generators (HIJING [10] and AMPT [11]) and GEANT [12] simulations of the detector response to determine the efficiency. The combined trigger and vertex reconstruction efficiencies for Cu + Cu collisions were found to be  $84 \pm 5\%$ ,  $75 \pm 5\%$ , and  $79 \pm 5\%$  for 200, 62.4, and 22.4 GeV, respectively. A small difference ( $\sim 5\%$  in determined efficiency) was found among methods, and this was considered in the final systematic uncertainty of the centrality determination. To optimize the efficiency and background levels for each dataset, the number of Paddles hit threshold was lowered from  $>2$  to  $>0$  for the 22.4-GeV data.

For this analysis, the centrality cross-section bin selection was based on the total energy deposited in the Octagon detector. As a cross-check of autocorrelation biases, the centrality bin selection was also determined by using the sum of energy in the Paddles, truncated to the 24 (of 32) lowest energy signal slats to remove Landau-tail fluctuations. No difference in the results between the two centrality methods was found for peripheral to mid-central data. A 3% difference was found only for the most central data point, which is covered by the systematic uncertainty on the measurement. The average number of participating nucleons,  $\langle N_{\text{part}} \rangle$ , for a given centrality bin was extracted from the initial Glauber-based values in the HIJING MC simulation for the associated centrality cuts on the final fully simulated Paddle and Octagon centrality distributions. Systematic uncertainties on  $\langle N_{\text{part}} \rangle$ , including the uncertainties in the efficiency of both triggering

and vertex reconstruction were determined by using different event generators. For more details on the PHOBOS centrality methods see Refs. [1,13].

The midrapidity charged-particle pseudorapidity density measurement in this Rapid Communication is based on hit patterns in the dual-plane Vertex silicon detector [9]. Two reconstructed hits in either the top or bottom pair of planes form a ‘‘tracklet.’’ Among all possible hit combinations, or tracklets, in these two detector planes, only those that point back to the predetermined vertex position (within a distance of closest approach of 6 mm) are utilized for the final measurement, greatly reducing the number of fake tracklet candidates. The charged-particle multiplicity is determined by counting the number of tracklet candidates and applying a correction factor to account for the geometrical acceptance of the detector, reconstruction efficiency, and vertex resolution [6]. Possible effects on the tracklet data, owing to the changing vertex resolution with multiplicity, were investigated with no systematic effects observed. The results were further checked for possible autocorrelation biases (owing to the new vertex reconstruction procedures) via comparison to the  $p_T$ -integrated invariant yields [14] and the single-layer analysis using the Octagon detector [15]. All results are found to be consistent.

The charged-particle pseudorapidity density, at midrapidity, scaled by the number of participating nucleon pairs is shown in Fig. 1 for Au + Au and Cu + Cu collisions. Figure 1(a) shows the published Au + Au data [7] and for each energy four new peripheral data points, with shaded error ellipses. The new Au + Au data (analyzed by using the techniques developed for Cu + Cu) extend the studies of charged particles at midrapidity from a fractional cross section of 50% to a peripheral value of 70%. The triggering and vertex reconstruction efficiency are 100% in this region. With these new peripheral data it is now apparent that the charged-particle multiplicities at midrapidity tend toward the inelastic  $p + p$  data. In addition, the new peripheral Au + Au data provide a large overlap in  $\langle N_{\text{part}} \rangle$  with the Cu + Cu data [Fig. 1(a)]. The Au + Au data points are also shown in Fig. 1(b) as a line, in comparison to the Cu + Cu data. The charged-particle yields are higher in Cu + Cu collisions than for inelastic  $p + p$  data, and, as for Au + Au collisions, the multiplicity per participant pair increases with centrality and collision energy. Within the systematic uncertainty, the trends in the centrality dependence of the charged-particle production are the same across systems. The degree to which the trends are the same is somewhat surprising in the context that the number of participants differ by a factor of 3 for the same cross-sectional fraction, owing to the much smaller size of the Cu nucleus. Previous studies [6] have shown that the fraction of hard collisions,  $x$ , obtained from a simple two-component parametrization applied to the data, is equivalent for both 19.6- and 200-GeV Au + Au collisions. Both results are consistent, within the systematic errors, with an averaged value of  $x = 0.13 \pm 0.01(\text{stat}) \pm 0.05(\text{syst})$ . Although some of the uncertainties could be attributed to the systematic errors on the data measurement, the striking data similarities across different energies and systems are better understood when ratios of data are taken.

A more precise way to look at trends in the data is to take ratios of the midrapidity charged-particle yields at different

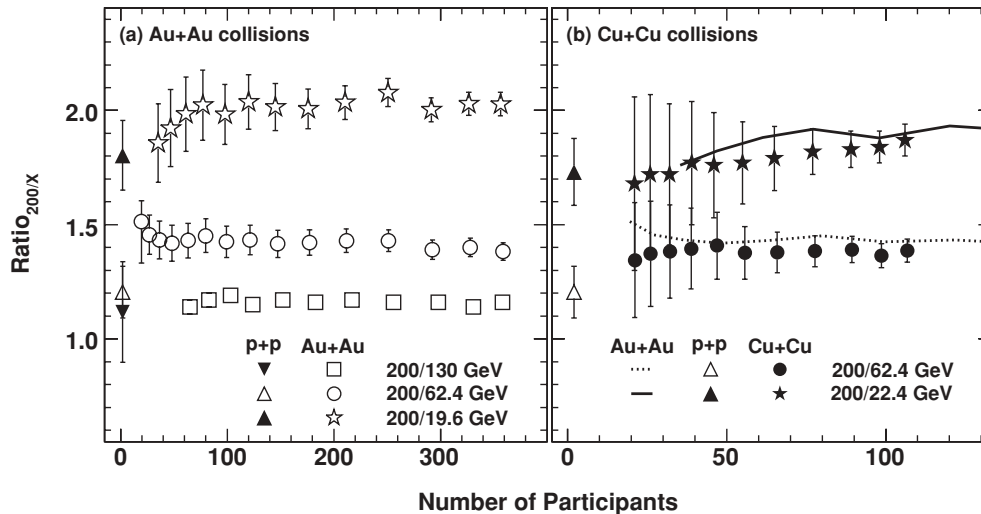


FIG. 2. The ratio between two collision energy datasets (200 GeV/ $X$  GeV) of the charged-particle pseudorapidity densities from Fig. 1. Panel (a) shows the data ratios from Au + Au collisions [7]. Panel (b) shows the Cu + Cu data, along with lines representing the Au + Au data (no errors) for comparison. In panel (b) the 19.6-GeV Au + Au data are scaled by 1.055 to account for the difference in collision energy between the low-energy Au + Au (19.6 GeV) and Cu + Cu (22.4 GeV) data. The triangles (at  $N_{\text{part}} = 2$ ) represent the inelastic  $p + p$  data at equivalent energies to the Au + Au data, as in Ref. [6]. Vertical error bars are combined statistical and systematic  $1\sigma$  uncertainties.

collision energies, as a function of centrality. In this way a large fraction of the systematic uncertainties in the measurement cancel, as detailed in Ref. [6], leaving a combined (statistical and systematic) uncertainty at the level of a few percent. The primary reason for this cancellation is that the analysis uses the same detector, reconstruction technique, triggering requirements, and centrality determination method across the different data samples. Systematic uncertainties arising from a common source are thus neutralized. The result of this analysis for all PHOBOS data on Au + Au and Cu + Cu collisions is shown in Fig. 2. These ratios are taken at the same fractional cross section for the two energies and shown versus the corresponding (averaged)  $N_{\text{part}}$  value. The small differences in  $\langle N_{\text{part}} \rangle$  for the same fraction of cross section for different collision systems has a negligible effect within a given collision system. Performing the analysis in the Au + Au system for precisely matched  $\langle N_{\text{part}} \rangle$  values yielded the same results [6]. Furthermore, the ratios obtained by using different centrality methods are consistent within the shown uncertainties.

We observe two striking features in the data. First, even within the reduced uncertainties, the slope of the ratios are consistent with zero for both Cu + Cu and Au + Au systems as a function of centrality. This observation in the data clearly illustrates that the factorization in centrality and collision energy of the midrapidity charged-particle yields is a feature of both the large Au + Au system as well as the smaller Cu + Cu system. As the ratios show no measurable centrality dependence, owing to the factorization into energy and centrality components, the trends of  $dN_{\text{ch}}/d\eta|_{|\eta|<1}$  with centrality seen in Fig. 1 are not driven by the collision energy, and thus they must be a consequence of the collision geometry (i.e., the volume of the interaction as defined by the number of participating nucleons). Second, we observe that the increase in charged-particle yields with collision energy is similar

between the Cu + Cu and Au + Au systems. In particular, the ratio of midrapidity charged-particle yields from 200 and 62.4 GeV are the same in Cu + Cu and Au + Au systems, within the systematic uncertainties.

The extent of the similarities in the charged-particle ratios for Cu + Cu and Au + Au collisions can be further tested by a comparative analysis of the inclusive charged-particle transverse momentum ( $p_T$ ) distributions. For this, data from Ref. [16] are used to form a ratio of charged-particle yields between  $\sqrt{s_{NN}} = 200$  and 62.4 GeV as functions of centrality and  $p_T$ . The results, shown in Fig. 3 for three bins of  $p_T$ , are independent of centrality, in agreement with those from the

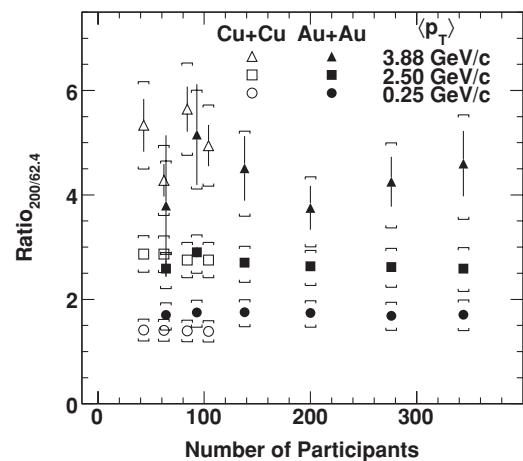


FIG. 3. Ratio (200 GeV/62.4 GeV) of charged-particle yields measured at three different  $\langle p_T \rangle$  values vs centrality in Au + Au (closed symbols) and Cu + Cu (open) collisions. Vertical error bars represent the statistical uncertainty in the measurement; brackets represent 90% C.L. systematic errors. The data are from Refs. [14,16,17].

bulk yields, even for transverse momenta up to  $p_T \sim 4 \text{ GeV}/c$ . One may expect that the produced yields at intermediate to high  $p_T$  would be predominantly formed from hard partonic collisions (i.e., those more likely to produce jets). As the hard collisions should follow a scaling with  $N_{\text{coll}}$  then a distinct  $N_{\text{part}}$  dependence of the ratio should be observed for different  $p_T$  ranges. In this regard, it is surprising to find no evidence of a centrality dependence apparent in the data at high  $p_T$ . The increase of the average ratio value with  $p_T$  is expected because of the harder spectra at 200 GeV compared to 62.4 GeV, as also observed in  $p + p$  collisions. A more definitive statement at high  $p_T$  would require data with higher statistics and lower systematic uncertainties.

It is important to point out that the effects observed in the  $p_T$  dependence favor a volume-dominated scenario of particle production, and it will be interesting to see whether the further differential measurements (particle-species-dependent effects) support this conclusion. Comparisons of proton to pion ratios in Au + Au collisions at 200 and 62.4 GeV are consistent with our observations for unidentified charged-particles [18]. From our study, it is clear that effects of multiple-nucleon collisions that strongly grow with centrality and energy play only a minor role, if any, in bulk charged-particle production.

In conclusion, we have reported new data for the midrapidity charged-particle density in Cu + Cu and peripheral Au + Au collisions at RHIC. The charged particle density per participant pair is found to be similar between peripheral Au + Au and Cu + Cu, for the same number of participants. The midrapidity yields of the smaller Cu + Cu system appear to factorize into collision-energy- and centrality-dependent components, in much the same manner as seen in the Au + Au system. The observed centrality independence of the ratios, between different center-of-mass energies, further illustrates that the collision volume ( $N_{\text{part}}$ ) drives the bulk yield of charged particle production at RHIC. This apparent general feature also appears to hold as a function of transverse momentum for  $p_T$  up to at least  $\sim 4 \text{ GeV}/c$ .

This work was partially supported by US DOE Grant Nos. DE-AC02-98CH10886, DE-FG02-93ER40802, DE-FG02-94ER40818, DE-FG02-94ER40865, DE-FG02-99ER41099, and DE-AC02-06CH11357, by US NSF Grant Nos. 9603486, 0072204, and 0245011, by Polish MNiSW Grant No. N N202 282234 (2008–2010), by NSC of Taiwan Contract No. NSC 89-2112-M-008-024, and by Hungarian OTKA Grant No. F 049823.

- 
- [1] B. B. Back *et al.* (PHOBOS Collaboration), Nucl. Phys. **A757**, 28 (2005).  
 [2] B. B. Back *et al.* (PHOBOS Collaboration), Phys. Rev. Lett. **88**, 022302 (2002).  
 [3] B. B. Back *et al.* (PHOBOS Collaboration), Phys. Rev. C **74**, 021902(R) (2006).  
 [4] D. Kharzeev and M. Nardi, Phys. Lett. **B507**, 121 (2001).  
 [5] B. B. Back *et al.* (PHOBOS Collaboration), Phys. Rev. C **65**, 061901(R) (2002).  
 [6] B. B. Back *et al.* (PHOBOS Collaboration), Phys. Rev. C **70**, 021902(R) (2004).  
 [7] B. B. Back *et al.* (PHOBOS Collaboration), Phys. Rev. C **74**, 021901(R) (2006).  
 [8] E. Garcia *et al.*, Nucl. Instrum. Methods A **570**, 536 (2007).  
 [9] B. B. Back *et al.*, Nucl. Instrum. Methods A **499**, 603 (2003).  
 [10] M. Gyulassy and X. N. Wang, Comput. Phys. Commun. **83**, 307 (1994). HIJING v1.383 was used.  
 [11] B. Zhang, C. M. Ko, B. A. Li, and Z. Lin, Phys. Rev. C **61**, 067901 (2000).  
 [12] GEANT Detector Simulation Tool v. 3.21, CERN (default parameters).  
 [13] R. S. Hollis *et al.* (PHOBOS Collaboration), J. Phys. G Conf. Series **5**, 46 (2005).  
 [14] B. Alver *et al.* (PHOBOS Collaboration), Phys. Rev. Lett. **96**, 212301 (2006).  
 [15] B. Alver *et al.* (PHOBOS Collaboration), Phys. Rev. Lett. **102**, 142301 (2009).  
 [16] B. B. Back *et al.* (PHOBOS Collaboration), Phys. Rev. Lett. **94**, 082304 (2005).  
 [17] B. B. Back *et al.* (PHOBOS Collaboration), Phys. Lett. **B578**, 297 (2004).  
 [18] B. I. Abelev *et al.* (STAR Collaboration), Phys. Lett. **B655**, 104 (2007).